Journal of Population Therapeutics & Clinical Pharmacology

RESEARCH ARTICLE
DOI: 10.53555/jptcp.v30i5.4067

ANTIMICROBIAL ACTIVITY, PHYSIOCHEMICAL AND SPECTRAL CHARACTERIZATION OF RARE EARTH METAL CHELATES BASED ON THIOCARBOHYDRAZIDE DERIVATIVES

Dr. Sharad Sankhe[1*], Mr. Shashank Parab[2]

[1*]Professor, Department of Chemistry, Patkar-Varde College, Goregaon West, Mumbai-62, India.
[2]PhD scholar, Department of Chemistry, Patkar-Varde College, Goregaon West, Mumbai-62, India

***Corresponding Author:** Dr. Sharad Sankhe
*Professor, Department of Chemistry, Patkar-Varde College, Goregaon West, Mumbai-62, India.

Abstract
The physiologically active N”-[(Z)-(4-Fluorophenyl)methylidene]-N”-[(1E,2E)-[hydroxylamine-1,2-diphenylidene]thiocarbohydrazide (HBMT*o*FB) ligand was prepared by condensation reaction between α-benzilmonoximethiocarbohydrazide and *o*-fluorobenzaldehyde in the presence of the catalytic amount of HCl. This ligand is used to synthesize lanthanide metal complexes. The kind of trinuclear lanthanide complexes [Ln(BMT*o*FB)$_3$]comprises ten different compounds. In this case, the functional groups of the synthesized Ln = La(III), Lu(III), Ce(III), Sm(III), Nd(III), Ho(III), Yb(III), Dy(III) Pr(III), and Gd(III) were shown in detail through UV-visible and infrared spectroscopy, PMR spectroscopy, elemental analysis (C, H, N, S analysis), magnetic susceptibility, and molar conductivity. Using powder XRD characteristics of the complexes were examined. N”-[(Z)-(4-Fluorophenyl)methylidene]-N”-[(1E,2E)-[hydroxylamine-1,2-diphenylidene] thiocarbohydrazide acted as a tridentate, monobasic ligand, and its two oxygen, two sulfur, and nitrogen atoms formed a structure that could interact with metal ions, according to infrared spectroscopy. The antibacterial activity of the synthesized metal complexes was successfully tested.

Keywords - Antimicrobial activity, biologically active molecule, Molar conductivity, Lanthanide complexes, Mononuclear.

INTRODUCTION:
The biological aspects of lanthanides have not been extensively studied, yet they seem to have intriguing pharmacological properties [1-3]. Undoubtedly, the lanthanides have been extensively examined and thoroughly characterized from a chemical perspective, offering intriguing prospects for future research in the forthcoming decades [4]. Metal ions are crucial in the mechanism of action of medicines [5]. They engage in distinct interactions with antibiotics, proteins, membrane constituents, nucleic acids, and other biomolecules [6-9]. Metal complexes can alter the toxicological and pharmacological effects of several drugs [10]. The metal that has received the most extensive research in this regard is the Gd(III) ion, which has demonstrated its usefulness in several therapies, including being a constituent of MRI contrast agents. The diverse chemical and magnetic characteristics of the lanthanide (III) ion-prepared lanthanide complexes are more important in cancer diagnostics and therapy. The study of lanthanides and their compounds has gained considerable importance in recent

years due to their significant applications in medical inorganic chemistry and materials research. Lanthanide complexes are employed as contrast agents in medicine for magnetic resonance imaging (MRI) and are increasingly significant in various diagnostic techniques and as radiotherapeutic medications [11-12]. The Lanthanide ions have excellent redox stability, which makes them highly ideal for use in cells when there are biological reducing agents such as ascorbate and thiols. Additionally, they have the advantage of favorable luminous qualities due to 4f↔5d, charge transfer, and f↔f transitions [13]. Researchers intrigued by the recent advancements in the field of medicinal chemistry are exploring the potential applications of lanthanides. These findings inspire us to investigate the coordination behavior of N”-[(Z)-(4-Fluorophenyl)methylidene]-N”-[(1E,2E)-[hydroxylamine-1,2-diphenylidene]thiocarbohydrazide (HBMT*o*FB) with lanthanide metal ions. This paper presents findings on the synthesis, characterization, and antibacterial properties of the ligand and its lanthanide metal complexes.

MATERIALS AND METHODS:

The chemicals and glassware used during the experimental procedure were of analytical standard. The metal nitrates of lanthanum (III), lutecium (III), cerium (III), holmium (III), ytterbium (III), dysprosium (III), samarium (III), and gadolinium (III), as well as the ligand o-fluorobenzaldehyde, were also of high purity. The solvents employed for recording spectra were of high quality and suitable for spectroscopic analysis. The bacterial species used for antibacterial screening included *Escherichia coli* (*E. coli*), *Pseudomonas aeruginosa* (*P. aeruginosa*), *Staphylococcus aureus* (*S. aureus*), and *Bascules subtilis* (*B. subtilis*). The bacterial species employed for antifungal screening included *Candida albicans* (*C. albicans*), and *Saccharomyces cerevisiae* (*S. cerevisiae*). The ligand and complexes were subjected to melting point determination and thin-layer chromatography (TLC) using a solvent mixture of hexane, and ethyl acetate in a 8:2 ml ratio. The recorded melting point of the ligand was 145.5 ˚C, but the melting temperatures of the complexes were higher than 360 ˚C. The conductivity was measured using a Zeal Tech conductometer with a cell constant of 1±10% cm^{-1}. The molar conductance was determined by utilizing 10^{-3} M solutions of metal chelates that were produced in a nitrobenzene solvent. The carbon and hydrogen microanalysis was conducted using the THERMO FINNIGAN CHNS analyzer. The concentrations of La(III), Lu(III), Ce(III), Sm(III), Nd(III), Ho(III), Yb(III), Dy(III) Pr(III), and Gd(III) were calculated using the EDTA back titration method [14]. The Bruker FT-IR spectrophotometer, operating in the range of 4000-400 cm^{-1}, was used to get Infrared spectra of inner transition complexes, as well as the ligand. The magnetic susceptibility of solid metal-ligand chelate complexes was determined using Gouy's method at a temperature of 293 K. $Hg[Co(CNS)_4]$ was used as a calibrant for the studies [15-17]. The electronic spectra of complexes were acquired using a JASCO V650 UV-vis spectrophotometer, which is a twin-beam instrument. The antibacterial activity of the synthesized complexes was evaluated by determining the minimal inhibitory concentrations using the Broth dilution methods [18].

EXPERIMENTAL:

Synthesis of HBMT*o*FB ligand:

The HBMT*o*FB ligand was synthesized using the condensation reaction of α-benzilmonoximethiocarbohydrazide (10 mmol) and *o*-fluorobenzaldehyde (10 mmol) in ethanol. The ultimate reaction mixture was subjected to reflux for a duration of 3 hours, subsequently cooled, and left undisturbed overnight at ambient temperature. Separate the yellow solid by passing it through a filter and rinse it with hot distilled water.

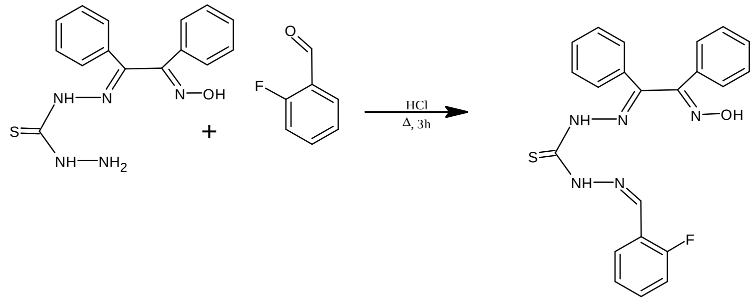

Scheme 1: Preparation of HBMT*o*FB ligand

Synthesis and metal complexes:

The metal complexes were synthesized by combining a 15 mmol metal nitrate solution with a 5 mmol HBMT*o*FB ligand solution prepared in ethanol. The stoichiometric ratio between the ligand and metal was 3:1. The reaction mixture underwent reflux for 3 hours at a temperature of 60°C. The reaction mixture was cooled and agitated for approximately 1 hour after 3 hours. No precipitation was detected at the moment. The pH of the reaction mixture was increased to 6.3 by adding a 0.1 M NaOH solution to create a virtually neutral environment for the precipitation of the complex. The precipitates of metal chelate that were produced in this manner were filtered and subsequently washed with alcohol to eliminate any remaining unreacted metal and ligand. The product underwent a drying process in an oven at a temperature of 50˚C. All the complexes were synthesized using the same procedure.

Antibacterial Screening:

By measuring the growth response of different microbes, we were able to determine the compounds' antibacterial properties. In vitro, using the disc diffusion method [20], we assessed the sensitivity of these microbes to growth rates of this kind.

To activate the bacterial strain activity, a 30 ml nutrient broth was injected with a loop full of the provided test strain and left to incubate in an incubator at 30 °C for 24 hours. 20 ml of the nutritional agar medium was applied to Petri dishes with a 120 mm diameter. When the media reached 37 °C, 0.1 ml of the activated strain was added to it. The media were given time to harden. Following the media's solidification, sterile filter paper discs (6 mm diameter) were placed in the Petri dishes for the sample and the standard drug kanamycin (30 µg/disc). As a control, we applied pure solvent to the discs in the Petri dishes and used a micropipette to apply the test samples under aseptic conditions. We repeated this process for each bacterial strain and solvent. A 24-hour incubation period at 37 °C was used for the Petri dishes.

To find out how effective the synthetic complexes were against the tested bacterial strain, researchers measured the inhibition zone that developed between the two chemicals. Consequently, the growth inhibition was determined by measuring the diameter of zones demonstrating complete inhibition (mm) in comparison to the positive control.

Minimum Inhibitory Concentration (MIC):

Using the same bacteria employed for antibacterial screening, the MIC of the test compounds was calculated using the serial tube dilution technique [18]. This was accomplished utilizing a nutritional agar medium. The test chemicals were diluted twofold in a serial fashion from the stock solution to create solutions with progressively lower concentrations.

Each tube was injected with 10 µl of a bacterial suspension that contained 10^7 cells/ml. After a day of incubation at 37 °C, the sample's MIC value in µg/ml was determined by removing the test tube from which no microorganism growth was apparent.

Brine shrimp lethality bioassay:

According to the protocol [19], the cytotoxic effects of the substances under investigation were investigated. For 48 hours, brine shrimp (*Artemia salina*) eggs were incubated in saltwater (made by mixing 38 g of NaCl with 1 liter of distilled water) at room temperature with continuous aeration. After diluting the compounds to 5 ml with seawater, stock solutions of the complexes (10 mg/ml in DMSO) were added to each vial, resulting in final concentrations of 0, 20, 40, 60, 80, and 100 µg/ml. Ten live shrimp were placed in each vial and left alone for one day. We counted and recorded the number of survived nauplii in each vial.

RESULTS AND DISCUSSION:

The ligand N”-[(Z)-(4-Fluorophenyl)methylidene]-N”-[(1E,2E)-[hydroxylamine-1,2-diphenylidene]thiocarbohydrazide (HBMT*o*FB) was used to synthesize complexes with La(III), Lu(III), Ce(III), Sm(III), Nd(III), Ho(III), Yb(III), Dy(III) Pr(III), and Gd(III) metal ions. These complexes were then characterized using various analytical methods. The complexes exhibit considerable solubility in DMSO and complete solubility in DMF, and nitrobenzene, whereas they are insoluble in methanol, ethanol, acetonitrile, and ethyl acetate. The complexes of La(III), Lu(III), Ce(III), Sm(III), Nd(III), Ho(III), Yb(III), Dy(III) Pr(III), and Gd(III) exhibit non-hygroscopicity. Gouy's approach was employed to conduct magnetic susceptibility measurements. The magnetic moment of lanthanide metal ions remains constant regardless of the ligands surrounding it, making it indistinguishable between different coordination geometries [20]. The molar conductance of metal complexes is being discussed. The value was discovered within the range of 0.259 to 1.428 $\Omega^{-1}cm^2mol^{-1}$. The presence of the mol^{-1} indication indicates that all the synthesized complexes are non-electrolytic.

Table-1: Analytical and physical data of the ligand and its lanthanide (III) metal complexes

Compound	Color	Yield %	M.P. / Dec. point°C	Elemental Analysis							Magnetic Moments (B.M.)	Electrical Conductance 10^{-3} M(in NB) mhos
				% M Found (Calcd)	% C Found (Calcd)	% H Found (Calcd)	% N Found (Calcd)	% O Found (Calcd)	% S Found (Calcd)	% F Found (Calcd)		
HBMT*o*FB	Yellow	86.97	187	-	62.99 (62.90)	4.33 (4.27)	16.70 (16.65)	3.81 (3.78)	7.64 (7.56)	4.53 (4.53)	-	-
[La(BMT*o*FB)$_2$]	Yellow	89.65	200	10.21 (10.32)	56.86 (56.78)	3.61 (3.65)	15.07 (15.03)	3.43 (3.41)	6.83 (6.80)	4.08 (4.08)	Dia	7.27
[Dy(BMT*o*FB)$_2$]	White	71.56	209	10.81 (10.77)	55.70 (55.91)	3.58 (3.60)	14.59 (14.83)	3.36 (3.39)	6.55 (6.78)	4.01 (4.02)	10.44	2.01
[Gd(BMT*o*FB)$_2$]	White	79.30	206	10.60 (10.65)	55.99 (56.12)	3.55 (3.61)	14.86 (14.88)	3.39 (3.40)	6.76 (6.80)	3.95 (4.00)	7.90	4.45
[Nd(BMT*o*FB)$_2$]	White	80.24	207	10.29 (10.32)	56.61 (56.64)	3.61 (3.65)	14.98 (15.02)	3.39 (3.43)	6.86 (6.87)	4.02 (4.08)	3.08	8.54
[Sm(BMT*o*FB)$_2$]	Yellow	79.65	209	10.71 (10.79)	56.33 (56.40)	3.59 (3.63)	14.91 (14.95)	3.40 (3.42)	6.81 (6.84)	4.04 (4.06)	3.60	10.11
[Lu(BMT*o*FB)$_2$]	Green	80.91	203	13.99 (14.03)	52.06 (52.23)	3.33 (3.36)	13.80 (13.85)	3.11 (3.17)	6.31 (6.33)	3.70 (3.76)	Dia	1.56
[Pr(BMT*o*FB)$_2$]	White	85.79	211	10.15 (10.20)	56.73 (56.78)	3.62 (3.66)	14.99 (15.05)	3.41 (3.44)	6.85 (6.88)	4.03 (4.09)	3.56	8.53
[Ce(BMT*o*FB)$_2$]	Yellow	91.22	206	10.02 (10.05)	52.74 (52.81)	3.62 (3.66)	15.00 (15.06)	3.43 (3.44)	6.79 (6.83)	4.02 (4.09)	1.83	6.68
[Ho(BMT*o*FB)$_2$]	L. Brown	83.61	213	14.09 (14.13)	52.26 (52.31)	3.52 (3.59)	14.32 (14.79)	3.36 (3.38)	6.73 (6.78)	4.01 (4.01)	10.37	5.39

IR spectra:

The ligand HBMT*o*FB binding mechanism to Ln(III) ions in these complexes was investigated by comparing the FT-IR spectrum of HBMT*o*FB with that of its Ln(III) complexes. The HBMT*o*FB ligand FT-IR spectrum exhibits two prominent absorption bands at 1718 cm^{-1} and 1187 cm^{-1}, corresponding to the (C=NN) and (C=NO) of the azomethine and oximino group, respectively. The infrared spectra of all Ln(III) complexes exhibited the characteristic bands of the ligand HBMT*o*FB, which were shown to shift in diverse ways as a result of complex formation. These shifts are documented in **Table 2**. The IR spectrum shifts of various complexes exhibit a resemblance, suggesting that the Ln(III) complexes possess comparable structures. The band detected at 3425 cm^{-1} in the IR spectra of the ligand corresponds to the stretching of the O-H bond. The metal-ligand

complexes of the disappearance of this band indicated that metal ions bonded via deprotonation of the oximino group.
The stretching vibrations of M-O, M←N, and M←S are attributed to the new bands observed in the complex IR spectra at 563-619, 530-577, and 506-533 cm^{-1}, respectively. The fact that these bands aren't present in the ligand spectrum proves that the metal ions in lanthanide HBMT*o*FB chelates are connecting with the azomethine nitrogen, thiocarbonyl sulfur, and oximino oxygen ions.

Table 2: IR spectral bands of the ligand (HBMT*o*FB) and its metal complexes (cm^{-1}):

Assignments	**HBMHoCB**	**La(III)**	**Ce(III)**	**Pr(III)**	**Nd(III)**	**Sm(III)**	**Gd(III)**	**Ho(III)**	**Yb(III)**	**Dy(III)**	**Lu(III)**
νOH Oximino	3387	-	-	-	-	-	-	-	-	-	-
N-H	3262	3261	3261	3261	3261	3262	3260	3261	3261	3260	3313
νCH	2977	2978	2978	2979	2979	2978	2977	2979	2978	2977	2835
νC=NN	1555	1514	1486	1514	1514	1514	1513	1514	1514	1515	1493
νC=NO	1511	1486	1459	1486	1488	1486	1485	1487	1488	1487	1467
νC=S	1246	1232	1232	1231	1232	1232	1231	1232	1232	1232	1235
νM-O	-	567	618	619	618	618	615	580	618	620	563
νM-N	-	535	572	577	577	567	563	537	577	575	530
νM→N	-	514	534	534	536	533	516	506	517	525	509

Electronic Spectral study:

Table 3 displays the UV-visible absorption spectrum data for the HBMT*o*FB ligand and its complexes, including the maximum absorption wavelength (λ_{max}) and the corresponding band assignment. The samples were produced with a concentration of 10^{-6} M using DMF as the solvent. The spectrum was then recorded at room temperature. The HBMT*o*FB ligand has two absorption peaks at 275 and 390 nm. The bands correspond to n→π* transitions resulting from the conjugation between the lone pair of electrons of sulfur atoms and the π electrons of the thiocarbonyl group (C=S). The La(III) complex exhibited absorption bands with broad but modest intensity in the visible range at 400-450 and 475-490 nm. These bands are attributed to charge transfer (CT) transitions of the L→M and M→L type between La(III) and the ligand. Additionally, there were other less strong bands observed between the wavelengths of 572 and 688 nm, which indicated the *d-d* transition of La (III) ($^2B_{1g}\rightarrow{}^2E_g$) [21]. Alternatively, the observed bands for the Sm(III) complex might be attributed to the 4*f*-4*f* transition. This transition occurs between the ground state $^6H_{5/2}$ and the excited states of $^4F_{3/2}$, $^4F_{9/2}$, $^6F_{11/2}$, and $^4G_{5/2}$ [22]. The gadolinium (III) complex exhibits *f-f* transition bands at wavelengths of 690 nm and 448.50 nm. These transitions correspond to the 4*f*-4*f* transition from the ground state $^8S_{7/2}$ to the excited states of $^6D_{5/2}$ [23].
The Ce(III) complex exhibited distinct absorption bands at 455 and 428 nm in its electronic spectra, suggesting a charge transfer phenomenon [24]. The magnetic moment of the Ce(III) complex is 1.83 B.M., which is lower than the values reported by Hund and Van-Vleck for Ln(III) and falls outside the standard experimental range of 2.14-2.46 B.M. [25-26]. The low values can be attributed to the antiferromagnetic interaction [27]. The narrow bands from 330 to 425 nm in the Dy(III) complex excitation spectrum are represented by $4f^9$ – intra-configurational transitions from the ground state $^6H_{15/2}$ to excited states $^4G_{9/2}$ (330 nm), $^4F_{5/2}$ + $^4D_{5/2}$ (341 nm), $^4M_{15/2}$ + $^6P_{7/2}$ (353 nm), $^4I_{11/2}$ (369 nm), $^4K_{17/2}$ (377 nm), $^4M_{19/2}$ + $^4M_{21/2}$ (390 nm), and $^4G_{11/2}$ (425 nm). As seen in Fig. 5f, the solid sample 4's emission spectra at room temperature after photo-excitation at 310 nm. The Dy(III) environment influences this hypersensitive emission peak at 572 nm [30]. Even in its solid form, the yellow emission was detectable, and it was much stronger than the blue.
As a result of spin-orbit coupling, the f^{10} modification of Ho^{3+} comprises 47 terms, resulting in 107 levels with varying values of *J*. The ground state of hydrogen ions is $^5I_8$. In the spectra of 370 to 680 nm, there were five obvious multiplet-to-multiplet conversions from the ground state to $^5F_2$ (Ho-III), $^5S_2$ and $^5F_4$ (Ho-IV), and $^5F_5$ (Ho-V) stimulated states for the Ho(III) complex. These conversions were given a ranking based on how often they occurred. The $^5G_6\rightarrow{}^5I_8$ centered absorption near 443 nm showed the most significant sensitivity to the ligand and solvent environment compared to all the other Ho^{3+} conversions observed in the study. It is possible to attribute the four emission peaks observed at 443, 486, 567, and 644 nm to the $^5G_3$ + $^3G_5\rightarrow{}^5I_8$, $^5G_6\rightarrow{}^5I_8$, $^5S_2$ + $^5F_4\rightarrow{}^5I_8$, and $^5F_5\rightarrow{}^5I_8$

transitions of the Ho^{3+} ion, respectively. Energy back-transfer from the Ho^{3+} ion became conspicuous in the ligand-centered emission band (490 nm) because there were inefficient transfers of energy from bpy to the Ho^{3+} center [29].

Transitions from the ground levels $^3H_4$ to the excited J levels of the $4f$ configuration cause the praseodymium (III) complex absorption bands in the UV and visible area to appear. The sharp bands caused by the *f-f* transition in the ^4f_n configuration of lanthanide ions are relatively unaffected by the metal ions near the vicinity. This is thought to be because the 4f orbitals are sheltered by the $5s^2$ and $5p^6$ orbitals that lie above. Nevertheless, it is reasonable to assume that complex formation is responsible for the transition to the lower frequency range [30].

The complexes exhibited a systematic red-shift in their electronic spectra, which can be attributed to the presence of covalent bonding. The UV-vis spectroscopic characteristics indicated the presence of covalent bonding between the hard lanthanide (III) ion and the soft ligands. Overall, the stoichiometry of the complexes can be determined as $[Ln(BMT\mathit{o}FB)_3]$. This determination is based on absorption spectra, magnetic characteristics, and chemical analysis.

NMR spectra:

It is reasonable to attribute the singlet seen at δ 12.436 ppm in the ligand's ^1H NMR spectra to the oximino proton. The spectral absence of this signal in diamagnetic lanthanum(III) complexes suggests that oximino oxygen plays a role in chelation following deprotonation [31]. Signals from aliphatic amine moiety protons and phenyl ring protons (two sets of singlets at δ 12.336 and 10.592 ppm) in the lanthanum(III) complexes' spectra do not show any change in their location. This indicates that the electrical environment around these sites, which are just a few bonds far from the metal ion, remains unaffected by the weak metal-ligand interactions.

Powder X-ray diffraction:

The extreme molecular mass of the metal ions prevented us from successfully producing single crystals of these complexes. This led to the recording of powder X-ray diffraction patterns. The diffraction patterns show the complex's crystalline nature. In the crystal structures of these complexes, efforts to index the diffraction patterns using autoindexing computer programs have yet to produce satisfactory unit-cell parameters. The massive chelate molecules caused a relatively larger unit cell and symmetry arrangements, which led to this.

According to the data shown above, complexes the metal ion through the oximino oxygen, thiocarbonyl sulfur, and azomethine nitrogen. The metal ion acquires a coordination number of nine. The lanthanide (III) complexes of N”-[(Z)-(4-Fluorophenyl)methylidene]-N”-[(1E,2E)-[hydroxylamine-1,2-diphenylidene]thiocarbohydrazide were suggested to have a monocapped trigonal prism shape according to the physicochemical and spectroscopic data that were collected.

Biological Activities:

Table 5 displays the results of the antibacterial activity of these compounds as determined by zone of inhibition. When tested against various harmful bacteria, the test compounds demonstrated high sensitivity. A standard medication disc containing 30 g of kanamycin was used to compare the results.

Compared to the conventional antibiotic kanamycin at a dose of 30 µg/disc, the potency of the Nd(III) complex against all test species was quite similar. When the complexes were tested with greater doses (100g/disc and 200g/disc), somewhat better results were observed. Even at large doses, the other three compounds, namely Sm(III), Pr(III), and Gd(III), had moderate action. No bacterial strain was inhibited by the solvent DMSO. The test drugs' MIC values, which are displayed in **Table 5**, were calculated in µg/ml.

The compounds' in vitro cytotoxic effect will be evaluated using the brine shrimp lethality assays. By analyzing the correlation between sample concentration and percentage of death, we were able to determine the median lethal concentration (LC_{50}) of brine shrimp lethality. According to the results, the LC_{50} values for Sm(III), Lu(III), Pr(III), and Ho(III) were 50, 45, 60, and 40µg/ml individually.

CONCLUSIONS:

These nine inner transition metal complexes of Schiff bases derived from N”-[(Z)-(4-Fluorophenyl)methylidene]-N”-[(1E,2E)-[hydroxylamine-1,2-diphenylidene]thiocarbohydra-zide are synthesized using a simple, rapid, and efficient procedure. **Figure 1** shows the structures that were suggested based on the nine coordinated geometries that were found in the aforementioned research. When it comes to metal complexes, thermal and IR data prove that the molecules are coordinated. The complexes are all non-electrolytic, have a color, and disintegrate at higher temperatures. The antimicrobial properties of all the synthetic chemicals have been studied. The newly synthesized compounds demonstrate a strong antibacterial action for the prepared compounds. It was discovered that all of these chemicals had cytotoxic effects. Hence, additional research using cutting-edge technology might lead to the development of these molecules as novel antibacterial drugs.

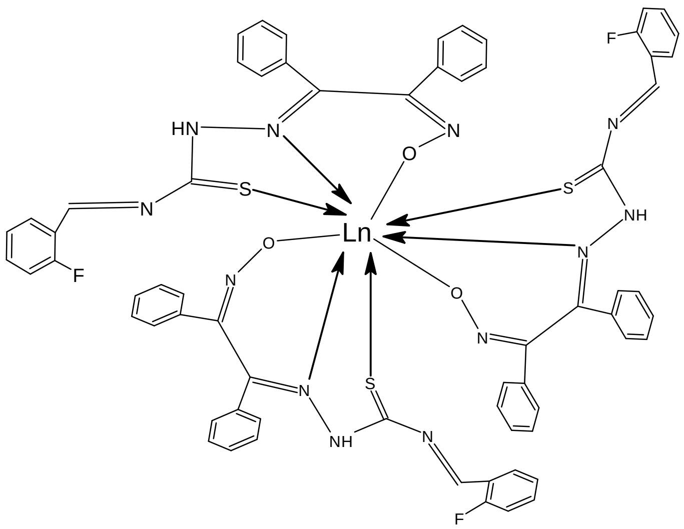

References:

1. Fouad, R. (2020). Synthesis and characterization of lanthanide complexes as potential therapeutic agents. *Journal of Coordination Chemistry*, *73*(14), 2015-2028.
2. Ajlouni, A. M., Abu-Salem, Q., Taha, Z. A., Hijazi, A. K., & Al Momani, W. (2016). Synthesis, characterization, biological activities and luminescent properties of lanthanide complexes with [2-thiophenecarboxylic acid, 2-(2-pyridinylmethylene) hydrazide] Schiff bases ligand. *Journal of rare earths*, *34*(10), 986-993.
3. Georgieva, I., Mihaylov, T., & Trendafilova, N. (2014). Lanthanide and transition metal complexes of bioactive coumarins: Molecular modeling and spectroscopic studies. *Journal of Inorganic Biochemistry*, *135*, 100-112.
4. Mishra, N., Kumar, K., Pandey, H., Anand, S. R., Yadav, R., Srivastava, S. P., & Pandey, R. (2020). Synthesis, characterization, optical and anti-bacterial properties of benzothiazole Schiff bases and their lanthanide (III) complexes. *Journal of Saudi Chemical Society*, *24*(12), 925-933.
5. Chundawat, N. S., Jadoun, S., Zarrintaj, P., & Chauhan, N. P. S. (2021). Lanthanide complexes as anticancer agents: A review. *Polyhedron*, *207*, 115387.
6. Staszak, K., Wieszczycka, K., Marturano, V., & Tylkowski, B. (2019). Lanthanides complexes–Chiral sensing of biomolecules. *Coordination Chemistry Reviews*, *397*, 76-90.
7. Mattocks, J. A., & Cotruvo, J. A. (2020). Biological, biomolecular, and bio-inspired strategies for detection, extraction, and separations of lanthanides and actinides. *Chemical Society Reviews*, *49*(22), 8315-8334.

8. Chundawat, N. S., Jadoun, S., Zarrintaj, P., & Chauhan, N. P. S. (2021). Lanthanide complexes as anticancer agents: A review. *Polyhedron*, *207*, 115387.
9. Shahraki, S., Shiri, F., Heidari Majd, M., & Dahmardeh, S. (2019). Anti-cancer study and whey protein complexation of new lanthanum (III) complex with the aim of achieving bioactive anticancer metal-based drugs. *Journal of Biomolecular Structure and Dynamics*, *37*(8), 2072-2085.
10. Chundawat, N. S., Jadoun, S., Zarrintaj, P., & Chauhan, N. P. S. (2021). Lanthanide complexes as anticancer agents: A review. *Polyhedron*, *207*, 115387.
11. Patyal, M., Kaur, K., Bala, N., Gupta, N., & Malik, A. K. (2023). Innovative Lanthanide Complexes: Shaping the future of cancer/tumor Chemotherapy. *Journal of Trace Elements in Medicine and Biology*, 127277.
12. Gill, M. R., & Vallis, K. A. (2019). Transition metal compounds as cancer radiosensitizers. *Chemical Society Reviews*, *48*(2), 540-557.
13. Wang, L., Zhao, Z., Wei, C., Wei, H., Liu, Z., Bian, Z., & Huang, C. (2019). Review on the electroluminescence study of lanthanide complexes. *Advanced Optical Materials*, *7*(11), 1801256.
14. Matharu, K., Mittal, S. K., & Kumar, S. A. (2011). A novel method for the determination of individual lanthanides using an inexpensive conductometric technique. *Analytical Methods*, *3*(6), 1290-1295.
15. Saunderson, A. (1968). A permanent magnet Gouy balance. *Physics Education*, *3*(5), 272.
16. Saha, N., & Bhattacharyya, D. (1976). Chelates of Cu (II), Ni (II) & Co (II) with 3, 5-Dimethylpyrazole-I-acetic Acid.
17. A. W. Bauer, W. M. M. Kirby, J. C. Sherries, M. Truck, Am. J. Clin. Path. 44 (1966) 493-497.
18. E. Jawetz, J. L. Melnick, E. A. Adelberg., Lange, Medical Pub. 14th ed., California, 1980, p. 123-124.
19. Atta-ur-Rahman, M. I. Choudhary, W. J. Thomsen., Harwood Academic Press, Amsterdam, 1999, p. 12-22.
20. Shebl, M., Khalil, S. M., & Al-Gohani, F. S. (2010). Preparation, spectral characterization and antimicrobial activity of binary and ternary Fe (III), Co (II), Ni (II), Cu (II), Zn (II), Ce (III) and UO2 (VI) complexes of a thiocarbohydrazone ligand. *Journal of Molecular Structure*, *980*(1-3), 78-87.
21. Ferenc, W., Cristóvão, B., & Sarzyński, J. (2013). Magnetic, thermal and spectroscopic properties of lanthanide (III) 2-(4-chlorophenoxy) acetates, Ln (C8H6ClO3) 3• nH2O. *Journal of the Serbian Chemical Society*, *78*(9), 1335-1349.
22. Wei, D. Y., Zheng, Y. Q., & Lin, J. L. (2002). Two Hydroxo Bridged Dinuclear Lanthanide Phen Complexes:[Ln2 (phen) 4 (H2O) 4 (OH) 2](phen) 2 (NO3) 4 with Ln= Tm, Yb. *Zeitschrift für Naturforschung B*, *57*(6), 625-630.
23. Al-Zaidi, B. H., Hasson, M. M., & Ismail, A. H. (2019). New complexes of chelating Schiff base: Synthesis, spectral investigation, antimicrobial, and thermal behavior studies. *Journal of Applied Pharmaceutical Science*, *9*(4), 045-057.
24. Guo, H., Wang, Y., Li, G., Liu, J., Feng, P., & Liu, D. (2017). Cyan emissive super-persistent luminescence and thermoluminescence in BaZrSi 3 O 9: Eu 2+, Pr 3+ phosphors. *Journal of Materials Chemistry C*, *5*(11), 2844-2851.
25. P. Singla, V. Luxami and K. Paul, Eur. J. Med. Chem., 2016, 117, 59
26. Jorgensen, C.K., Prog. Inorg. Chem., 1962, vol. 4, p. 73.
27. Silverstein, R.M., Bassler, G.C., and Morrill, T.C., Spectrometric Identification of Organic Compounds, New York: Wiley, 1981.